Measurements of the static polarizability of the $8s\ ^2S_{1/2}$ state of atomic cesium

D. Antypas[1] and D. S. Elliott[1,2]

[1]*Department of Physics, Purdue University, West Lafayette, Indiana 47907, USA*

[2]*School of Electrical and Computer Engineering, Purdue University, West Lafayette, Indiana 47907, USA*

(Received 25 February 2011; published 20 June 2011)

We present improved measurements of the static polarizability of the $8s\ ^2S_{1/2}$ state of atomic cesium. Measured separately on two hyperfine components of the $6s\ ^2S_{1/2} \rightarrow 8s\ ^2S_{1/2}$ transition, we determine an average polarizability of $\alpha_{8s} = 9.490 \pm 0.012$ MHz $(\mathrm{kV/cm})^{-2}$, and a difference of only $\Delta\alpha_{8s} = 0.014 \pm 0.016$ MHz $(\mathrm{kV/cm})^{-2}$. α_{8s} is consistent with, but of higher precision (<0.15%) than, the previous measurement and theory. The difference $\Delta\alpha_{8s}$ is smaller than our previous determination, and within 1 σ of zero. Our new technique is insensitive to the frequency calibration of the laser.

DOI: 10.1103/PhysRevA.83.062511 PACS number(s): 32.10.Dk, 32.60.+i, 32.10.Fn

I. INTRODUCTION

We recently reported a measurement of the static polarizability α of the $8s\ ^2S_{1/2}$ state of atomic cesium [1]. We carried out this measurement on the two hyperfine components ($F = 3 \rightarrow F' = 3$ and $F = 4 \rightarrow F' = 4$) of the two-photon $6s\ ^2S_{1/2} \rightarrow 8s\ ^2S_{1/2}$ transition. The average polarizability that we reported, $\alpha_0 = 38\,060 \pm 250\ a_0^3$, was in good agreement with the theoretical value, $\alpha_0 = 38\,260 \pm 290 a_0^3$, reported in that same work [1]. We also noted a small difference, $\sim 0.8\%$, in the measured value of α on the $F = 3 \rightarrow F' = 3$ and $F = 4 \rightarrow F' = 4$ transitions. The accompanying theory did not address the hyperfine state dependence of α.

It is known that a small difference in the atomic polarizability can be induced by the hyperfine interaction between the electronic angular momentum and the nuclear spin. Feichtner *et al.* [2] calculated this Stark shift on the hyperfine splitting of the cesium ground state, and determined that the transition frequency of this 9.1926-GHz line varies as $-1.9 \times 10^{-6}\ E_0^2$ Hz $(\mathrm{V/cm})^{-2}$, where E_0 is the dc field amplitude. The magnitude of the difference, $\alpha(F = 4) - \alpha(F = 3)$, associated with this variation is quite small, amounting to only $\sim 1.2 \times 10^{-5}$ of the average polarizability of the ground state. In applying their analysis technique to calculate the hyperfine-coupling-induced value of the $\alpha(F = 4) - \alpha(F = 3)$ for the $8s$ state, we arrive at a similarly small estimate, $\sim 5 \times 10^{-6}$ of the average polarizability of the $8s$ state. Thus there is no theoretical basis for the 0.8% difference reported in Ref. [1].

A finite hyperfine dependence of the static polarizability, if it were real, would imply the possibility that related quantities such as the scalar and vector polarizabilities (that quantify the amplitude of Stark-induced electric dipole interactions on transitions that are dipole forbidden in the absence of a dc electric field) differ with the hyperfine component as well. The vector polarizability β of the $6s\ ^2S_{1/2} \rightarrow 7s\ ^2S_{1/2}$ transition has played a central role in determination of the electroweak parity-nonconserving interaction amplitude $\mathrm{Im}(\mathcal{E}_{\mathrm{PNC}})$ [3]. Here the 4.8% difference of the measured ratio $\mathrm{Im}(\mathcal{E}_{\mathrm{PNC}})/\beta$ on different hyperfine components of the transition has inferred a large anapole moment of the Cs nucleus. Implicit in these conclusions is the lack of any hyperfine dependence of β. For this reason, we have returned to our measurements of the Stark shift in cesium, with the goal of re-examining the difference in the static polarizability of the two hyperfine components of the $8s$ state.

In the following section, we describe the measurement technique, followed by a discussion of the results and conclusions.

II. EXPERIMENT

The technique that we employ for the measurement of the Stark shift was adapted from the work of van Wijngaarden and Li [4]. It relies on imposing rf sidebands onto the laser beam, and exciting atoms in a field-free reference cell with the laser sideband while concurrently exciting the Stark-shifted atoms in a separate region with the laser carrier. By determining the sideband frequency at which the two resonances occur simultaneously, we are able to measure the Stark shift without requiring a precise calibration of the laser scan frequency. A schematic of our apparatus is shown in Fig. 1. Light from a frequency-stabilized cw Ti:sapphire laser tuned to the $6s\ ^2S_{1/2}, F = 3 \rightarrow 8s\ ^2S_{1/2}, F' = 3$, or $F = 4 \rightarrow F' = 4$ two-photon transition ($\lambda = 822.46$ nm) excites the atoms. We measure the Stark-shifted resonance in an atomic beam inside a vacuum chamber, which simplifies the construction and placement of highly parallel field plates. The reference resonance is provided by Cs atoms in a separate field-free vapor cell. After passing through the interaction region, each of the two optical beams is reflected back on itself, resulting in Doppler-free resonances for the atoms when the laser frequency is scanned. The spectra of the reference and the Stark-shifted resonance are recorded by collecting the fluorescence at 794.6 nm with photomultiplier tubes (PMT) as the atoms decay to the $6p\ ^2P_{3/2}$ state. Using an electro-optic modulator (EOM) positioned between the Cs cell and the reflector, we phase modulate the return laser beam going through the vapor cell at a frequency ν_m, imposing sidebands at frequencies $\nu_L \pm n'\nu_m$, where $n' = 1, 2, \ldots$ and ν_L is the carrier frequency. One of the resonances in the reference cell occurs at $\nu_L + (\nu_L + \nu_m) = (E_{8s} - E_{6s})/h$, where E_{8s} (E_{6s}) is the unshifted energy of the $8s$ ($6s$) state and h is Planck's constant. The resonance in the Stark-shifted atomic beam occurs at $2\nu_L = (E_{8s} - E_{6s})/h - kE_0^2 - \nu_{\mathrm{off}}$, where $k = \frac{1}{2}(\alpha_{8s} - \alpha_{6s})$ is the Stark shift coefficient, and α_{8s} (α_{6s}) is the static polarizability of the $8s$ ($6s$) state. ν_{off} is a small residual Doppler shift occurring from imperfect overlap of

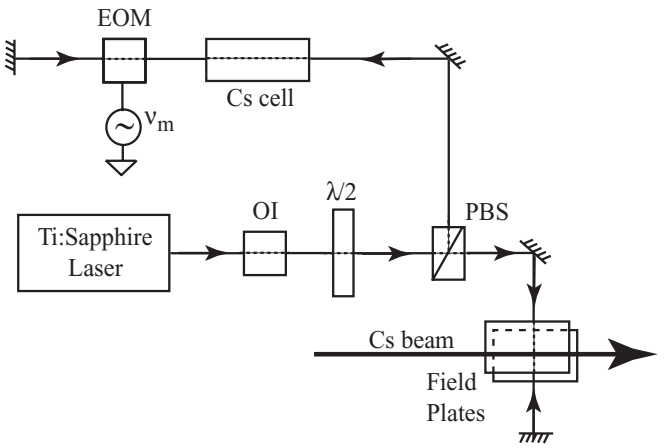

FIG. 1. Experimental configuration for the Stark shift measurements. Narrow-band tunable light at $\lambda = 822$ nm is tuned through the two-photon transition frequency, and the excitation signal in the Stark-shifted atom beam and the reference cell recorded concurrently. Phase modulation of the reference beam in the electro-optic modulator (EOM) imposes sidebands at frequency ω_m on that beam. Other abbreviations in this diagram are as follows: OI, optical isolator; $\lambda/2$, half-wave optical retarder; PBS, polarizing beam splitter.

the counterpropagating beams intercepting the atomic beam. We designate the modulation frequency that causes the two resonances to occur at the same carrier frequency ν_L as $\nu_m(0)$, where

$$\nu_m(0) = kE_0^2 + \nu_{\text{off}}. \tag{1}$$

We measure k by determining values of $\nu_m(0)$ for six different electric field strengths E_0 and fitting Eq. (1) to the data.

We maintain the temperature of the reference vapor cell at 70°C, corresponding to an atomic density of 2×10^{12} cm^{-3}. We focus the laser beam into the vapor cell, where the beam waist radius is ∼45 μm. After passing through an EOM, the beam is reflected back on itself, and retraces the path of the incident beam. The line shape of the two-photon absorption resonance consists of a sharp [$\Delta\nu_h \sim 4.6$ MHz full width at half maximum (FWHM)] Doppler-free peak on top of a very low-level Doppler-broadened ($\Delta\nu_D \sim$ GHz) background. (The background is highly suppressed relative to the Doppler-free peak by the ratio $\Delta\nu_h/\Delta\nu_D$, and we can model the background as frequency independent over the spectral region of interest.) The 4.6-MHz linewidth of the transition that we observe in the reference cell is somewhat greater than the 1.8-MHz natural linewidth of the 6S-8S transition [6]. This difference can be partly attributed to transit time broadening, which we estimate to be 1.5 MHz, occurring due to the focused optical beams in the interaction region.

We measure the Stark-shifted resonance in an atomic beam, which we generate with an effusive heated stainless steel oven, fitted with a nozzle that consists of a pack of stainless steel capillary tubes, patterned after Ref. [5]. At an oven temperature of 120°C, the nozzle creates a relatively collimated beam with an estimated density of 10^{10} cm^{-3} in the interaction region. Before reaching the interaction region, atoms pass through a rectangular aperture of width 1 cm and height 0.3 cm, which helps reduce the residual Doppler broadening [measured to be 20 MHz (FWHM) from Gaussian fits to single pass spectra of the $6S \rightarrow 8S$ two-photon transition] and prevents coating of the electric field plates with cesium. The field plates are transparent, consisting of a 100-nm-thick layer of indium tin oxide (ITO) on glass microscope slides of dimensions 2.54 cm wide by 7.62 cm long. They are spaced by 0.6436(4) cm with the use of eight ceramic spacers. We estimate the variation in the spacing of the glass slides to be $\Delta d/d \sim 6 \times 10^{-4}$, as judged by the relative ease with which we can slip calibrated ceramic beads, whose lengths we measured to ± 2.5 μm, between the plates at various locations, similar to the technique described in Ref. [7]. Numerical computation of the static field for this configuration shows that the field variation within the interaction region due to fringing effects is limited to less than a part in 10^5. The choice of transparent plates allows for efficient collection of fluorescence photons by an aspheric lens (2-inch focal length, 3-inch diameter) placed above the upper plate. We use a set of interference filters to reduce the scattered light reaching the PMT. With the lower plate grounded, we apply a potential of up to 2.5 kV to the upper plate. We measure this voltage using a calibrated voltage attenuator (Tektronix model P6015 010-0131-00, attenuation factor 1005.9:1) and a precision volt meter. Voltages in excess of 2.5 kV cause drifts in the attenuated voltage, which are most likely the result of heating in the attenuator. For the range of applied voltages these drifts are always less than 1 part per 10^4. The line shape of this two-photon absorption resonance consists of a Doppler-free central component, superposed on a Doppler-broadened background. The linewidth of the Doppler-free peak is typically 4.9 MHz. We believe that this is mostly limited by

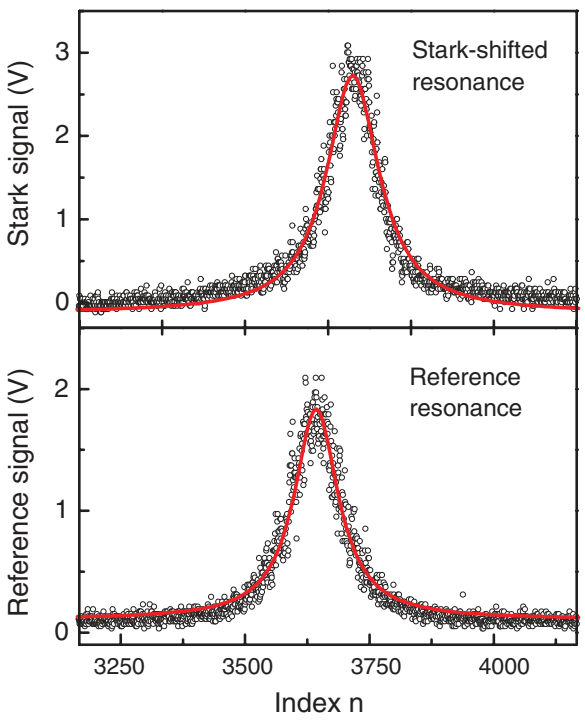

FIG. 2. (Color online) Recorded spectra of the reference and Stark-shifted resonance, corresponding to excitation from the first-order sideband and the carrier frequency, respectively. The lines represent Lorentzian curves fitted to the data.

transit-time broadening (∼2.9 MHz) and lifetime broadening. The amplitude of the Doppler-broadened background is only about 15% of the peak height of the Doppler-free resonance. We align the laser beam to be perpendicular to the beam direction in order to minimize the asymmetry of the Doppler-broadened background. With this careful alignment, we find that fitting the absorption resonance with a single Lorentzian line shape provides a good fit to the data.

We carry out separate measurements for the $F = 3 \rightarrow F' = 3$ and $F = 4 \rightarrow F' = 4$ transitions as follows: We first adjust E_0 to yield a Stark shift of approximately 25 MHz. With the electric field value held constant we then sweep the laser frequency (100 MHz scan length in 2.5 s) and record the two-photon spectra for $\nu_m = 22$ MHz to $\nu_m = 28$ MHz, in increments of 1 MHz. We show a typical set of spectra of the reference and Stark-shifted resonances in Fig. 2. Each spectrum consists of $n_{\max} = 6250$ data points (0.4 ms of integration per data point). We fit Lorentzian curves to these spectra to determine the position of the peaks to an uncertainty of approximately 10 kHz, and the peak separation Δn_{peak}. (Throughout the course of these measurements, we use the data point index n in place of the direct frequency calibration. The frequency scan of the laser is, to a close approximation, linear in time, so the frequency step size in these scans is approximately 100 MHz/$n_{\max}$ = 16 kHz.)

III. ANALYSIS

In Fig. 3, we show a plot of the measured peak separations Δn_{peak} as a function of modulation frequencies for $E_0 = 2.238$ kV/cm. The solid line represents a linear fit to the data; the corresponding fit residuals appear in the lower panel. From this fit we determine the frequency $\nu_m(0)$ that corresponds to a zero peak separation. The rms deviation of these data is around $\Delta n = 2.5$, corresponding to approximately 40 kHz, which we believe is largely due to a slight pointing instability of our laser beam. Such an instability would cause drifts in the residual Doppler shift of the Stark-shifted resonance. The observed 40-kHz fluctuations correspond to a change in the angle between the (nominally) counterpropagating beams in the interaction region as small as 15 μrad. We saw a decrease in the residual values after we decreased the length of the beam path from the laser to the interaction region, supporting our suspicion of the pointing instability. It must be noted that this pointing instability does not shift our reference resonance, since the atomic velocities in the vapor cell are isotropic; it only affects the Doppler broadening slightly.

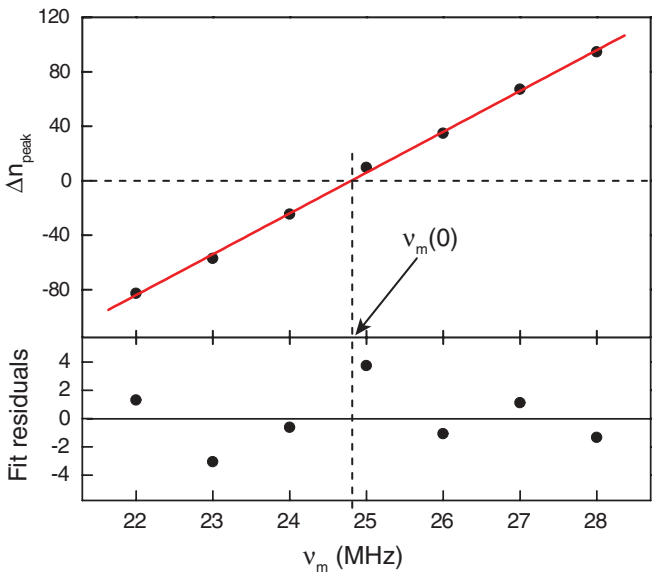

FIG. 3. (Color online) Modulation frequency versus peak separation and residuals from the straight line fitted to the data.

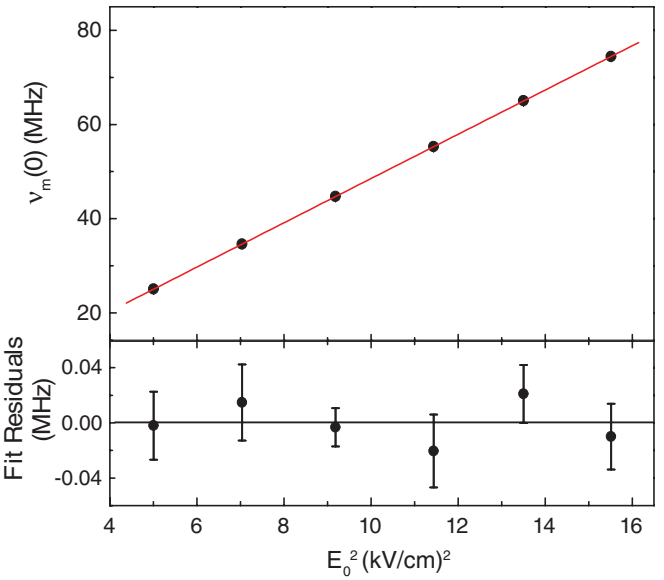

FIG. 4. (Color online) Modulation frequency corresponding to zero peak separation as a function of electric field for the $F = 4 \rightarrow F' = 4$ transition, along with a linear fit to the data and the corresponding fit residuals. The slope of the straight line fit to the data yields the Stark shift.

We carry out the measurements described above at six different values of E_0, corresponding to Stark shifts of about 25 MHz through 75 MHz, in increments of 10 MHz. We show a plot of $\nu_m(0)$ versus E_0^2 in Fig. 4. The Stark shift coefficient k is the slope of the straight line fitted to this data, using Eq. (1). We repeat the determinations of $k(F = 3 \rightarrow F' = 3)$ and $k(F = 4 \rightarrow F' = 4)$ on two successive days, with results shown in Table I. We also present in this table the frequency offset ν_{off} from each of the fits. The uncertainties that we quote for these four individual determinations represent the

TABLE I. The Stark shift coefficients k and the frequency offsets ν_{off} for individual data sets, and the average value of k for the $F = 3 \rightarrow F' = 3$ and $F = 4 \rightarrow F' = 4$ transitions. The uncertainties are discussed in the text.

		k[MHz/(kV/cm)^2]	ν_{off} (MHz)
$F = 3$	Day 1	4.6936 ± 0.0019	1.58 ± 0.02
$\rightarrow F' = 3$	Day 2	4.6890 ± 0.0014	1.51 ± 0.02
	Average	4.691 ± 0.006	
$F = 4$	Day 1	4.6949 ± 0.0029	1.30 ± 0.03
$\rightarrow F' = 4$	Day 2	4.7007 ± 0.0020	1.52 ± 0.02
	Average	4.698 ± 0.006	

TABLE II. The uncertainties that contribute to the uncertainties in the final determinations of $k(F = 3 \rightarrow F' = 3)$ and $k(F = 4 \rightarrow F' = 4)$.

Source of error	Symbol	relative magnitude
Field plate separation	$\Delta d/d$	6×10^{-4}
Volt meter	$(\Delta V/V)_V$	8×10^{-5}
Attenuator heating	$(\Delta V/V)_{\text{att}}$	$<8 \times 10^{-5}$
Power supply ripple	$(\Delta V/V)_R$	$<3 \times 10^{-5}$
Fringe field effects	$\Delta E_0/E_0$	$\sim 0.3 \times 10^{-5}$
Attenuator calibration	$\Delta G/G$	1.4×10^{-6}
Frequency generator	$\Delta f/f$	$\sim 10^{-5}$
Statistical	$\Delta f/f$	$\sim 10^{-5}$

statistical uncertainty of the fit to the data points. For each fit, the value of χ^2 is close to 1, indicating that a straight line provides a good fit to the data. The values of ν_{off} are relatively small ($\sim$1.5 MHz), and consistent to within $\pm$ 0.15 MHz over the course of the measurements.

The individual values of $k(F = 3 \rightarrow F' = 3)$ differ by $\sim$0.1%, or 0.0046 MHz/(kV/cm)^2, slightly larger than the combined error bars of 0.0033 MHz/(kV/cm)^2, but less than the uncertainty due to other experimental factors, as discussed in the following, similarly for $k(F = 4 \rightarrow F' = 4)$.

We list in Table II the uncertainties in various experimental parameters that can affect our determination of the Stark-shift coefficient, along with our estimate of the relative magnitude of each. The primary source of uncertainty in our measurements is the field plate spacing, d. If the plates are perfectly flat and the spacing between plates perfectly uniform, then we expect the static field E_0 to be perfectly uniform at any location between the plates, provided that we avoid the edges of the field plates where the electric field fringe effects start to play a role. At the level of accuracy of our measurements, effects that occur when the plates are less than perfect start to become important. If the local plate spacing varies, then the local field strength also varies, and measuring the Stark shift of cesium atoms in that space will reflect the local value of the static field E_0. For this reason, alignment can affect the measurement value. Since the Stark shift scales as E_0^2, and E_0 varies as $1/d$, the 0.06% variation in d can lead to a 0.12% variation in the Stark shift, consistent with the variation we observe in k, and which could result from the day-to-day realignment of the laser beams, for example. Other experimental factors that could affect the determination of k are also given in Table II; our estimates of these magnitudes indicate that they have little effect on our measurements. The net relative error in our measurement, which we calculate from the quadrature sum of the individual errors, is less than 0.15%, or 0.006 MHz/(kV/cm)^2. This is the uncertainty in the average value of the Stark shift coefficient that we report in Table I.

We return now to one of our primary motivations for carrying out these improved measurements of the Stark shift on this transition, that is, to determine the difference in polarizability for the two hyperfine components of the transition. We report $\Delta k = 0.007 \pm 0.008$ MHz/(kV/cm)^2, where the uncertainty is the quadrature sum of the uncertainties of the average values of $k(F = 3 \rightarrow F' = 3)$ and $k(F = 4 \rightarrow F' = 4)$. Thus, to within the 0.15% accuracy of our measurements, the observed difference in the Stark shift is consistent with 0, in contrast to our previous measurements [1]. We believe that small differences in the calibration of the laser frequency scan in the previous measurements may have been responsible for the previous nonzero result.

Using the average Stark shift from Table I, $k = 4.695 \pm 0.006$ MHz/(kV/cm)^2 and the ground-state polarizability 401 $a_0^3 = 0.0998$ MHz (kV/cm)$^{-2}$ [8], we determine the average polarizability of the $8s\,^2S_{1/2}$ state to be $\alpha_{8s} = 9.490 \pm 0.012$ MHz (kV/cm)$^{-2}$, or 38 110 $\pm$ 50 a_0^3. This is an improvement over the experimental value $\alpha_{8s} = 38\,060 \pm 250\ a_0^3$ that we reported in Ref. [1]. Our result is also in good agreement with the theoretical result of Safronova and Safronova $\alpha_{8s} = 38\,260 \pm 290\ a_0^3$ reported in Ref. [1]. The difference in polarizability for the two hyperfine components is $\Delta\alpha_{8s} = 0.014 \pm 0.016$ MHz (kV/cm)$^{-2}$.

ACKNOWLEDGMENTS

We are happy to acknowledge the assistance of Jintao Zhang with the electric field computations, and the support of the National Science Foundation under Grant No. PHY-0970041 during the final stages of this work.

[1] M. Gunawardena, D. S. Elliott, M. S. Safronova, and U. Safronova, Phys. Rev. A **75**, 022507 (2007).
[2] J. D. Feichtner, M. E. Hoover, and M. Mizushima, Phys. Rev. A **137**, 702 (1965).
[3] C. S. Wood, S. C. Bennett, D. Cho, B. P. Masterson, J. L. Roberts, C. E. Tanner, and C. E. Wieman, Science **275**, 1759 (1997).
[4] W. A. van Wijngaarden and J. Li, Phys. Rev. A **55**, 2711 (1997).
[5] V. Gerginov and C. E. Tanner, Optics Commun. **222**, 17 (2003).
[6] J. Marek, Phys. Lett. A **60**, 190 (1977).
[7] J. Li and W. A. van Wijngaarden, Phys. Rev. A **51**, 3560 (1995).
[8] J. M. Amini and H. Gould, Phys. Rev. Lett. **91**, 153001 (2003).